Available online at www.sciencedirect.com

SciVerse ScienceDirect

Ceramics International 38 (2012) 3829–3834

CERAMICS INTERNATIONAL

www.elsevier.com/locate/ceramint

Investigation of transport behavior in Ba doped $BiFeO_3$

A.R. Makhdoom [a], M.J. Akhtar [b], M.A. Rafiq [a,*], M.M. Hassan [a]

[a] Department of Metallurgy and Materials Engineering, PIEAS Nilore, Islamabad, Pakistan
[b] Physics Division, PINSTECH, P.O. Nilore, Islamabad, Pakistan

Received 28 September 2011; received in revised form 23 December 2011; accepted 12 January 2012
Available online 21 January 2012

Abstract

$Bi_{1-x}Ba_xFeO_3$ ($x = 0.00$–0.25) samples were prepared by conventional solid state reaction method. X-ray diffraction revealed the rhombohedrally distorted perovskite structure for undoped $BiFeO_3$ with a phase transition from rhombohedral to pseudo cubic on Ba substitution. The leakage current density of 10% Ba substituted sample is found to be four orders of magnitude less than that of the pure $BiFeO_3$. Grain boundary limited conduction and space charge limited conduction mechanisms are involved in low and high electric field regions respectively for all the samples except 10% Ba doped $BFeO_3$ which obeys grain boundary limited conduction mechanism in whole of the electric field range. Dielectric measurements showed that the dielectric constant and dielectric loss attained their minimum values at 10% Ba substitution. Thus 10% Ba is found to be optimum concentration to have better multiferroic properties. Undoped $BiFeO_3$ and 5% Ba doped samples have very large values of dielectric constants and leakage current densities which can be attributed to a large number of oxygen vacancies in these samples, indicating an extrinsic response of these compositions.

Keywords: B. Grain size; B. Porosity; Multiferroics; Leakage current density

1. Introduction

Ferroelectric, ferromagnetic and ferroelastic behaviors of the materials are very useful from application point of view. The materials exhibiting at least two out of the above three behaviors simultaneously are known as multiferroics [1–3]. Among the various types of multiferroics, $BiFeO_3$ has attracted much attention of researchers due to its promising potential applications in the fields of electromagnetic coupling, spintronics, sensors and data storage devices [4–7]. In $BiFeO_3$, ferroelectric and anti-ferromagnetic ordering coexist in a single phase at room temperature, that is, dielectric properties can be controlled by applied magnetic field and magnetization can be controlled by varying electric field [8]. $BiFeO_3$ has rhombohedrally distorted ABO_3 type perovskite structure with space group R3c [9]. It has high ferroelectric Curie temperature $T_C \sim 1103$ K and G-type anti-ferromagnetic Néel temperature $T_N \sim 643$ K [10]. Ferroelectricity appears in pure $BiFeO_3$ due to off centered distortion of Fe^{3+} ions, caused by 6 s^2 lone pair of Bi^{3+} ions in its noncentrosymmetric rhombohedral structure [11]. $BiFeO_3$ has canted spins structure that generates localized antiferromagnetism which is suppressed by the spiral spin structure at macroscopic level [12].

Large number of oxygen vacancies produced due to highly volatile nature of Bi and the multiple oxidation states of Fe (Fe^{2+} and Fe^{3+}) cause a high leakage current in the material that degrades its ferroelectric properties. On the other hand, the localized ferromagnetism produced by the canting of spins in $BiFeO_3$ vanishes at macroscopic level due the spiral spin structure of the magnetic domains with a wavelength ~620 Å. Due to these limitations $BiFeO_3$ has restricted applications. Several researchers have worked to overcome these limitations by synthesizing nanostructures or thin films of $BiFeO_3$ using appropriate synthesis technique and/or by doping rare earth metals/lanthanides at A site and/or transition elements at B site. Kawae et al. [13] codoped $BiFeO_3$ with Mn and Ti and found greatly reduced leakage current and high remnant polarization of 75 $\mu C/cm^2$ when they applied an electric field of 2100 kV/cm. Qian et al. [14] found a large magneto-dielectric coefficient of 4.7% in as-prepared $BiFeO_3$ nanoparticles. Yang et al. [15] found a great enhancement in magnetization with Co^{2+} substitution for Fe^{3+} ions. Wang et al. [16] studied the

* Corresponding author. Tel.: +92 51 2208014; fax: +92 51 2208070.
E-mail address: fac221@pieas.edu.pk (M.A. Rafiq).

0272-8842/$36.00
doi:10.1016/j.ceramint.2012.01.032

magnetic and ferroelectric properties of Ba doped $BiFeO_3$. In the present work, we replaced Bi^{3+} ions with Ba^{2+} to modify the structure and transport properties of $BiFeO_3$. We observed anomalous variations in leakage current density and dielectric properties with increasing Ba concentration and discussed their origin.

2. Experimental

Pure and Ba doped $BiFeO_3$ polycrystalline samples of the type $Bi_{1-x}Ba_xFeO_3$ ($x = 0.00, 0.05, 0.10, 0.15, 0.20, 0.25$) were synthesized by conventional solid state reaction method. Stoichiometric amounts of Bi_2O_3, Fe_2O_3 and $BaCO_3$ having 99.9% purity were thoroughly mixed and ground in a pestle and mortar for 30 min for each composition. The calcinations of the ground powders were carried out at temperatures of 750 °C and 800 °C for the time duration of 20 h, with an intermediate grinding for 30 min. Then the powders were ground and pressed into pellets having diameter ~9 mm and thickness ~1 mm and sintered at 825 °C.

In order to confirm the phase purity of the synthesized samples, XRD data was collected using D8 Discoverer HR-XRD BRUKER (Germany) with CuK_α radiations ($\lambda = 1.5418$ Å). The XRD data was collected in $15^\circ \leq 2\theta \leq 70^\circ$ range with a step size of 0.02° and count rate of 2 s/step. Scanning electron microscopy (SEM) was carried out to observe the microstructure of the synthesized samples. For electrical measurements the opposite flat faces of the pellets were coated with silver paste to make them a parallel plate capacitor and cured at 150 °C for 1 h. Room temperature dielectric measurements were carried out using Agilent E4980A LCR meter in the frequency range from 20 Hz to 2 MHz. The response of the current density, J, to applied electric field, E, was analyzed using Keithley 2400 Source Meter.

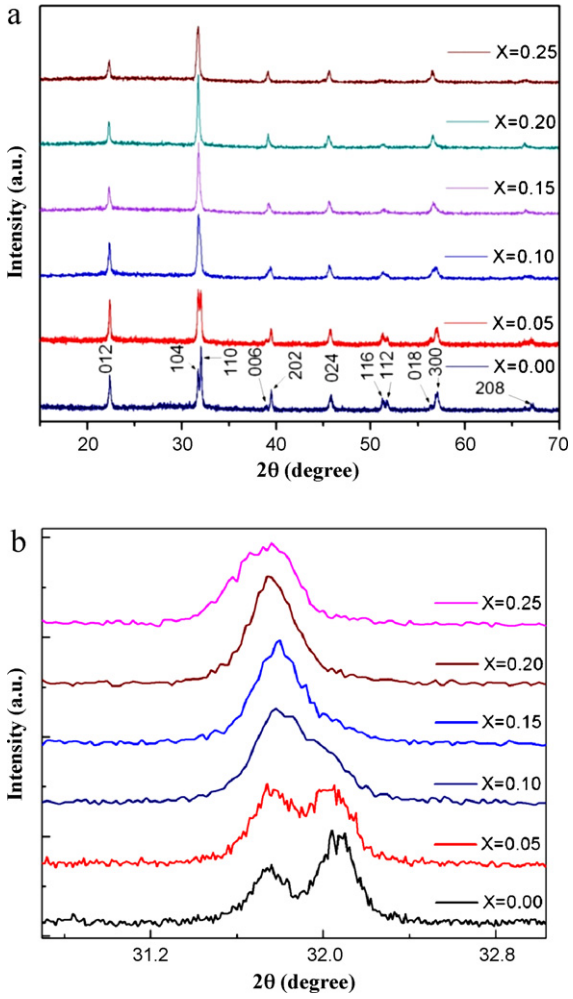

Fig. 1. (a) XRD pattern of the samples $Bi_{1-x}Ba_xFeO_3$ ($x = 0.00$–0.25), (b) Enlarged view of the diffraction peaks (1 0 4) and (1 1 0) near diffraction angle $2\theta = 32^\circ$.

3. Results and discussions

Fig. 1(a) shows the XRD patterns of $Bi_{1-x}Ba_xFeO_3$ ($x = 0.00$–0.25) samples recorded at room temperature. All the diffraction peak positions for $BiFeO_3$ polycrystalline match well with those of the rhombohedral R3c structure [17,18] with no impurity peak. The diffraction peak positions for Ba doped $BiFeO_3$ show gradual variations in peaks when compared with parent $BiFeO_3$. Doubly split peaks near 32°; (1 0 4) and (1 1 0), near 37°; (0 0 6) and (2 0 2) and near 52°; (1 1 6) and (1 1 2) merge gradually. This shows a structural phase transition from distorted rhombohedral to pseudo cubic symmetry. This behavior has also been reported for Pb substitution at Bi site in $BiFeO_3$ [19]. Fig. 1(b) shows the enlarged portion between 2θ of 31° and 33°, where mergence of (1 0 4) and (1 1 0) peaks is evident. All diffraction peaks shift slightly towards low angle indicating an increase in lattice parameters [20] caused by substitution of Ba atoms with larger ionic radius (1.42 Å) in place of Bi atoms having smaller ionic radius (1.17 Å).

In Fig. 2, SEM images demonstrate the effects of Ba concentration in $BiFeO_3$ on the grain size and porosity of the samples. It is clear from Fig. 2 that the average grain size is greatly reduced from 5 μm to 100 nm with increasing Ba concentration. However for 15% Ba, the grain size is slightly increased. This may be due to the structure phase transition from rhombohedral to pseudo cubic structure as confirmed by the XRD pattern. It has been suggested that the grain growth depends upon the concentration of oxygen vacancies [21] and diffusion rate of the ions. Due to highly volatile nature of Bi, its evaporation generates large number of oxygen vacancies in pure $BiFeO_3$. This makes it easy for the ions to diffuse, resulting in a very large grain size as compared to the Ba doped $BiFeO_3$ samples. This phenomenon may be suppressed by the occupation of certain probable evaporated Bi sites by Ba ions at low doping level. Although, on further Ba doping oxygen vacancies are generated for charge neutralization, but grain growth is limited due to substitution of Ba atoms with larger ionic radius in place of Bi atoms having smaller ionic radius.

To investigate the leaky behavior of the $Bi_{1-x}Ba_xFeO_3$ ($x = 0.00$–0.25) system, these materials were subjected to the electric field up to 400 V/cm at room temperature and leakage current densities were measured against varying electric field. In Fig. 3, it is demonstrated that current density increases with

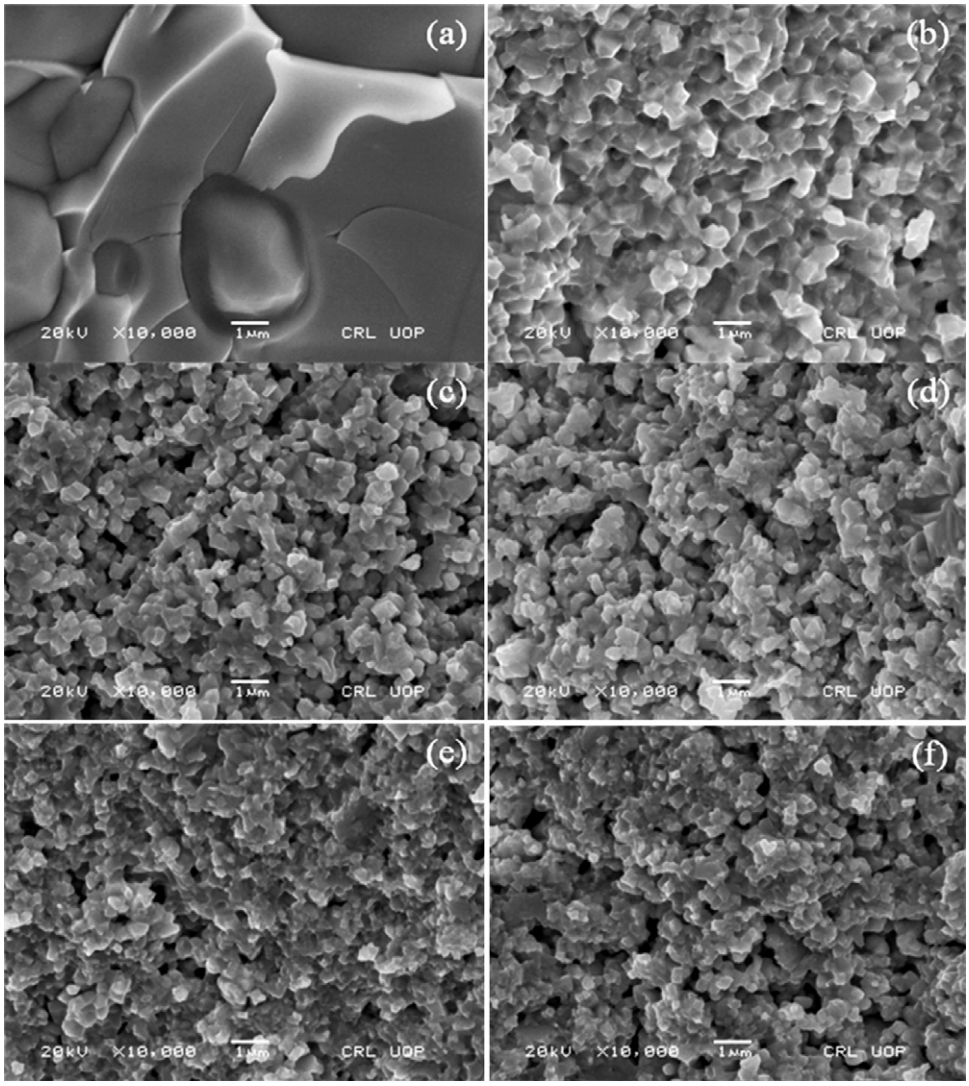

Fig. 2. SEM photographs of the samples $Bi_{1-x}Ba_xFeO_3$, (a) $x = 0.00$, (b) $x = 0.05$, (c) $x = 0.10$, (d) $x = 0.15$, (e) $x = 0.20$ and (f) $x = 0.25$, sintered at 825 °C.

increase in electric field for all compositions. When considering the effects of Ba concentration on the leakage current density, it is clear from Fig. 3 that 5% Ba doping has no considerable effect on leakage current density but doping of 10% Ba in $BiFeO_3$ reduces its leakage current density up to four orders of magnitude as compared to pure $BiFeO_3$. This makes a significant improvement in ferroelectric properties of the material. On further increase in Ba concentration, leakage current density first increases up to 20% and then decreases for 25% Ba contents. This behavior has also evidence in tan δ versus frequency measurements as discussed later. Hu et al. [22] have reported similar behavior for Gd doped $BiFeO_3$. Although, the transport behavior of $BiFeO_3$ system is very complicated but there are primarily three possible factors that control the transport properties. First is the concentration of oxygen vacancies [20,23] produced due to highly volatile nature of Bi. These oxygen vacancies generate deep trap energy levels within the band gap and provide a path for thermally or electrically stimulated charge carriers to flow under applied electric field. This phenomenon has direct correspondence with the leakage current density. Second is the multiple oxidation states of Fe ions (Fe^{2+} and Fe^{3+}) [7,24–26]. This behavior of Fe contributes to the conduction at high electric field by the transfer of the electrons from Fe^{2+} to Fe^{3+}, that is, virtual hopping of the Fe^{2+} takes place in the vicinity of high electric field. Thus, a high concentration of Fe^{2+} ions in the material gives rise to high leakage current [26]. The third factor that significantly affects the leaky behavior of $BiFeO_3$ system is the microstructure, i.e. volume of the grains and grain boundaries and density of the material. It is a well known fact that decrease in the grain size increases the grain boundary region and hence, increases the resistivity of the material [12,25,27,28]. Therefore, large number of oxygen vacancies, high concentration of Fe^{2+} ions, large grain size and more compact structure give rise to the leaky behavior in the $BiFeO_3$ system. The anomalous leaky behavior, as shown in Fig. 3, can be estimated by considering these factors. The substitution of Ba^{2+} for Bi^{3+} may cause two parallel phenomena with respect to concentration of oxygen vacancies, one is decrease in concentration of oxygen vacancies by filling the probable vacant volatized Bi^{3+} sites and

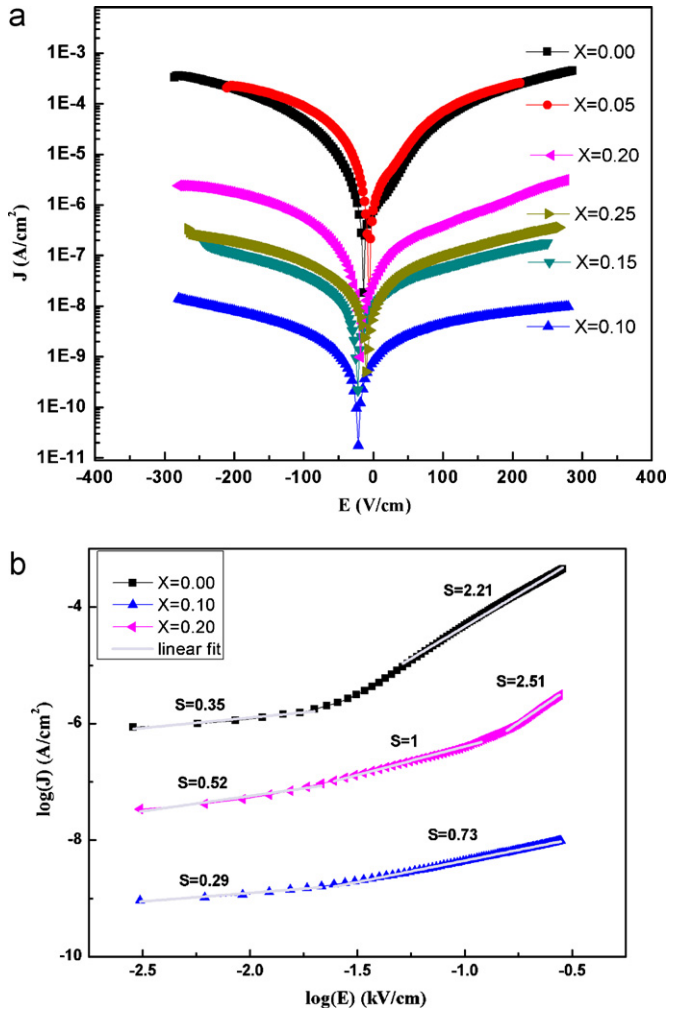

Fig. 3. (a) Leakage current density, J, vs. electric field, E, and (b) log(J) vs. log(E) plot for the samples $Bi_{1-x}Ba_xFeO_3$ ($x = 0.00$–0.25).

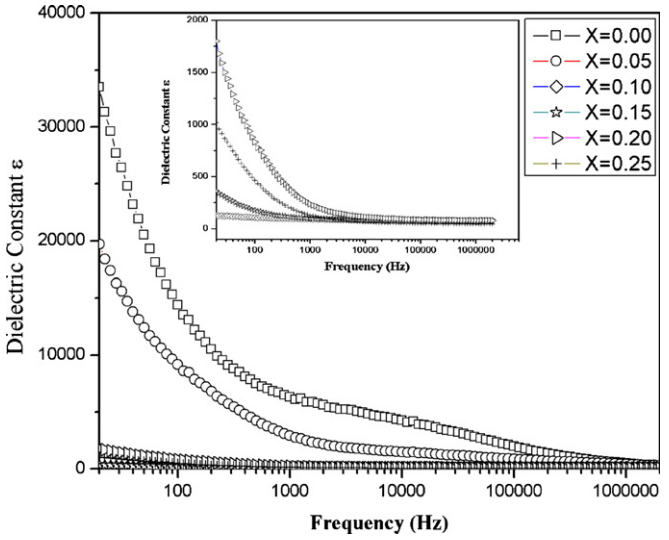

Fig. 4. Frequency response of dielectric constant for the samples $Bi_{1-x}Ba_xFeO_3$ ($x = 0.00$–0.25).

the second is the creation of oxygen vacancies to neutralize the charge produced by substituting Ba^{2+} for Bi^{3+}. Hence, we may consider a decrease in number of oxygen vacancies in low doping level up to 10% Ba and then an increase in oxygen vacancies concentration on further doping. Thus, greatly reduced leakage current density for 10% Ba is due to decrease in grain size (shown in Fig. 2), and reduction in concentration of Fe^{2+} ions and oxygen vacancies related defects [29,30]. For 15% Ba, grain size as well as oxygen vacancies concentration are slightly increased due to relatively large substitution of Ba as discussed earlier, the current density is found to be increased. Although, grain size of the 20% Ba doped sample is decreased slightly as compared to 15% Ba but the microstructure is more compact (less pores) and oxygen vacancies concentration also increases which may results in increase in the leakage current density. For 25% Ba doped sample, leakage current density is slightly decreased due to comparatively large porosity in the structure as indicated in Fig. 2.

Ohmic conduction (when bulk charge density is larger than the density of injected charges form the electrode) and the space-charge-limited conduction (when density of injected charges form the electrode is larger than that of the charges in the bulk) mechanisms are commonly involved in the transport behavior of $BiFeO_3$ ceramics. Logarithmic plot of the current density, 'J' and electric field, 'E' is a useful tool to find the conduction mechanism involved in leakage behavior of the samples. Based on the power law $J \alpha E^m$ relationship, we plotted log(J) versus log(E) in Fig. 3(b) for three selected samples with $x = 0.00$, 0.10 and 0.20. The value of slope 'm' for a specific region of these curves gives the information about the conduction mechanism involved in that region [26]. In the low electric field region the value of slope of the curves is less than unity for all the samples indicating grain boundary limited conduction [31]. In the high electric field region, the value of slope for undoped and 20% Ba doped $BiFeO_3$ is greater than 2 ($m > 2$) which shows that the space-charge-limited conduction (SCLC) is dominant for undoped and 20% Ba doped $BiFeO_3$ [26]. In the samples with $x = 0.15$–0.25, same conduction mechanisms are involved as that of 20% Ba doped $BiFeO_3$ (not shown here). However, for 10% Ba doped sample, it is less than unity ($m < 1$), indicating that the grain boundary limited conduction is dominant for this sample. This is expected due to reduced concentration of charge defects (oxygen vacancies, impurity phases, etc.) in this sample. However, for intermediate values of electric field, the slope of the curve for 20% Ba doped sample is 1 ($m = 1$) indicating an Ohmic conduction mechanism in this sample intermediate electric fields.

The above investigation about the existence of charge defects predicts large values of dielectric constant for pure and 5% Ba doped $BiFeO_3$. Fig. 4 shows dielectric measurement of the samples $Bi_{1-x}Ba_xFeO_3$ ($x = 0.00$–0.25) in the wide frequency range from 20 Hz to 2 MHz at room temperature. The dielectric constant ε has maximum values at the lower frequencies for all samples which decrease sharply with increasing frequency up to about 1 kHz and then become almost constant at high frequencies. It shows a large dielectric dispersion due to the Maxwell–Wanger type of interfacial (ionic and dipole) polarization. The reason is that the larger size and mass of dipoles can respond to only low frequencies but at

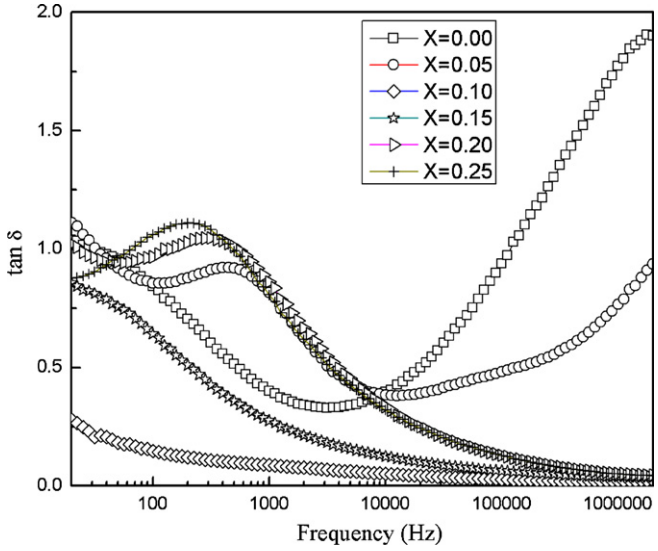

Fig. 5. Frequency response to the dielectric loss for the samples $Bi_{1-x}Ba_xFeO_3$ ($x = 0.00$–0.25).

high frequencies they are unable to be in step with the frequency of the applied electric field and relaxed down [12]. This behavior is common in dielectric and ferroelectric materials [32]. The dielectric constant as well as its frequency dependent region change systematically with doping concentration. Very large values of dielectric constant at low frequencies for pure and 5% Ba doped $BiFeO_3$ samples are observed. This may be attributed to the interfacial polarization due to high concentration of oxygen vacancies which are produced due to highly volatile nature of Bi, and/or multiple oxidation states of iron (Fe^{3+} and Fe^{2+}) [29]. It is an extrinsic behavior of these samples which is suppressed with further increase in Ba concentration. The inset shown in Fig. 4 is an enlarged view of dielectric measurements for 10% Ba and higher concentrations. The sample with 10% Ba substitution shows lowest value of dielectric constant due to reduced grain size [33] and low concentration of charge defects (oxygen vacancies and Fe^{2+}) [30]. On further doping, the value of dielectric constant becomes larger due to increase of oxygen vacancies. However for 25% Ba dielectric constant is reduced due to significant replacement of Bi^{3+} with Ba^{2+} ions; which is responsible for ferroelectricity in these materials [24].

The dielectric loss tan δ shows strong frequency dependence as indicated in Fig. 5. For all concentrations, tan δ has high values in the low frequency region that decrease gradually with increase in frequency. For $x = 0.00$ and 0.05, a second Deby like relaxation peak appears which can be attributed to the relaxation of charge carrier trapped among the oxygen vacancies. This ionic relaxation is a high frequency phenomenon that originates from thermally activated hoping of ions generated due to these oxygen vacancies. The value of relaxation frequency in tan δ measurements helps to predict the relative mobility of the charge carriers [34]. In the present study, the relaxation peak shifted towards higher frequency for 5% Ba sample indicates relatively high mobility. However, it is shifted towards very low frequency for 10% Ba showing very low mobility (reduced leakage current). On further increase in Ba concentration up to 20%, the relaxation peak is again shifted towards high frequency predicting the high leakage current. For 25% Ba contents, it is shifted again towards low frequency indicating low leakage current. Thus, the tan δ relaxation peak shift towards the lowest frequency for 10% Ba doped sample also confirms its lowest mobility as compared to other samples. These results are well consistent with the findings discussed for leakage current density measurements.

4. Conclusions

Polycrystalline samples with formula $Bi_{1-x}Ba_xFeO_3$ ($x = 0.00$–0.25) were synthesized by conventional solid state reaction method. XRD diffraction confirms the structural phase transition from rhombohedral to pseudo cubic symmetry. Anomalous variations are observed in dielectric and transport properties with Ba substitution that may be attributed to charge defects and variation of grain size. The leakage current density of 10% Ba doped sample is about four orders of magnitude less than those of pure $BiFeO_3$ sample. Small values of leakage current density and dielectric loss tan δ of 10% Ba doped $BiFeO_3$ make it an important multiferroic material.

Acknowledgement

We acknowledge Higher Education Commission (HEC) of Pakistan for the financial support in Ph.D. research of A.R. Makhdoom.

References

[1] N.A. Hill, Why are there so few magnetic ferroelectrics? J. Phys. Chem. B 104 (2000) 6694–6709.
[2] W. Eerenstein, N.D. Mathur, J.F. Scott, Multiferroics and magnetoelectric materials, Nature 442 (2006) 759–765.
[3] T. Kimura, T. Goto, H. Shintani, K. Ishizaka, T. Arima, Y. Tokura, Magnetic control of ferroelectric polarization, Nature 426 (2003) 55–58.
[4] J. Wang, J.B. Neaton, H. Zheng, V. Nagarajan, S.B. Ogale, Epitaxial $BiFeO_3$ multiferroic thin film heterostructures, Science 299 (2003) 1719–1722.
[5] H. Bea, M. Bibes, M. Sirena, G. Herranz, K. Bouzehouane, Combining half-metals and multiferroics into epitaxial heterostructures for spintronics, Appl. Phys. Lett. 88 (2006) 062502–62504.
[6] Y-H. Lin, Q. Jiang, Y. Wang, C-W. Nan, L. Chen, J. Yu, Enhancement of ferromagnetic properties in $BiFeO_3$ polycrystalline ceramic by La doping, Appl. Phys. Lett. 90 (2007) 172507–172509.
[7] Y. Wang, C-W. Nan, Enhanced ferroelectricity in Ti-doped multiferroic $BiFeO_3$ thin films, Appl. Phys. Lett. 89 (2006) 052903–52905.
[8] A.A. Belik, T. Furubayashi, Y. Matsushita, M. Tanaka, S. Hishita, E. Takayama-Muromachi, Indium-based perovskites: a new class of near-room-temperature multiferroics, Angew. Chem. Int. Ed. 48 (2009) 6117–6120.
[9] V.E. Demidov, S.O. Demokritov, G. Reiss, K. Rott, Enhancement of ferromagnetic properties in $BiFeO_3$ polycrystalline ceramic by La doping, Appl. Phys. Lett. 90 (2007) 172507–172509.
[10] J. Liu, L. Fang, F. Zheng, S. Ju, M. Shen, Enhancement of magnetization in Eu doped $BiFeO_3$ nanoparticles, Appl. Phys. Lett. 95 (2009) 022511–22513.
[11] V.A. Khomchenko, D.A. Kiselev, J.M. Vieira, A.L. Kholkin, M.A. Sa, Y.G. Pogorelov, Synthesis and multiferroic properties of $Bi_{0.8}A_{0.2}FeO_3$ (A = Ca,Sr,Pb) ceramics, Appl. Phys. Lett. 90 (2007) 242901–242903.

[12] P. Uniyal, K.L. Yadav, Study of dielectric, magnetic and ferroelectric properties in $Bi_{1-x}Gd_xFeO_3$, Mater. Lett. 62 (2008) 2858–2861.
[13] T. Kawae, Y. Terauchi, H. Tsuda, M. Kumeda, A. Morimoto, Improved leakage and ferroelectric properties of Mn and Ti codoped $BiFeO_3$ thin films, Appl. Phys. Lett. 94 (2009) 112904–112906.
[14] F.Z. Qian, J.S. Jiang, S.Z. Guo, D.M. Jiang, W.G. Zhang, Multiferroic properties of $Bi_{1-x}Dy_xFeO_3$ nanoparticles, J. Appl. Phys. 106 (2009) 084312–84318.
[15] Y. Wang, G. Xu, L. Yang, Z. Ren, X. Wei, W. Weng, P. Du, G. Shen, G. Han, Enhanced ferromagnetic properties of multiferroic $BiCo_{x-}Fe_{1-x}O_3$ synthesized by hydrothermal method, Mater. Lett. 62 (2008) 3806–3808.
[16] D.H. Wang, W.C. Goh, M. Ning, C.K. Ong, Effect of Ba doping on magnetic, ferroelectric, and magnetoelectric properties in mutiferroic $BiFeO_3$ at room temperature, Appl. Phys. Lett. 88 (2006) 212907–212909.
[17] P. Uniyal, K.L. Yadav, Observation of the room temperature magnetoelectric effect in Dy doped $BiFeO_3$, J. Phys.: Condens. Matter 21 (2009) 012205–12209.
[18] S.U. Lee, S.S. Kim, H.K. Jo, M.H. Park, J.W. Kim, A.S. Bhalla, Electrical properties of Cr-doped $BiFeO_3$ thin films fabricated on the p-type Si(1 0 0) substrate by chemical solution deposition, J. Appl. Phys. 102 (2007) 044107–44112.
[19] X. Zhang, Y. Sui, X. Wang, J. Tang, W. Su, Influence of diamagnetic Pb doping on the crystal structure and multiferroic properties of the $BiFeO_3$ perovskite, J. Appl. Phys. 105 (2009), 07D918-2.
[20] B. Yu, M. Li, J. Liu, D. Guo, L. Pei, X. Zhao, Effects of ion doping at different sites on electrical properties of multiferroic $BiFeO_3$ ceramics, J. Phys. D: Appl. Phys. 41 (2008) 065003–65007.
[21] K. Brinkman, T. Iijima, K. Nishida, T. Katoda, H. Funakubo, The influence of acceptor doping on the structure and electrical properties of sol–gel derived $BiFeO_3$ thin films, Ferroelectrics 357 (2007) 35–41.
[22] G.D. Hu, X. Cheng, W.B. Wu, C.H. Yang, Effects of Gd substitution on structure and ferroelectric properties of $BiFeO_3$ thin films prepared using metal organic decomposition, Appl. Phys. Lett. 91 (2007) 232909–232911.
[23] Z. Yan, K.F. Wang, J.F. Qu, Y. Wang, Z.T. Song, S.L. Feng, Processing and properties of Yb-doped $BiFeO_3$ ceramics, Appl. Phys. Lett. 91 (2007) 082906–82908.
[24] J. Liu, M. Li, L. Pei, J. Wang, Z. Hu, X. Wang, X. Zhao, Effect of Ce and Zr codoping on the multiferroic properties of $BiFeO_3$ thin films, Europhys. Lett. 89 (2010) 57004–57010.
[25] J. Liu, M. Li, L. Pei, B. Yu, D. Guo, X. Zhao, Effect of Ce doping on the microstructure and electrical properties of $BiFeO_3$ thin films prepared by chemical solution deposition, J. Phys. D: Appl. Phys. 42 (2009) 115409–115415.
[26] X. Qi, J. Dho, R. Tomov, M.G. Blamire, J.L. MacManus-Driscoll, Greatly reduced leakage current and conduction mechanism in aliovalent-ion-doped $BiFeO_3$, Appl. Phys. Lett. 86 (2005) 062903–62905.
[27] Y. Wang, C-W. Nan, Effect of Tb doping on electric and magnetic behavior of $BiFeO_3$ thin films, J. Appl. Phys. 103 (2008) 024103–24108.
[28] M. Idrees, M. Nadeem, M. Atif, M. Siddique, M. Mehmood, M.M. Hassan, Origin of colossal dielectric response in $LaFeO_3$, Acta Mater. 59 (2011) 1338–1346.
[29] F. Azough, R. Freer, M. Thrall, R. Cernik, F. Tuna, D. Collison, Microstructure and properties of Co-, Ni-, Zn-, Nb- and W-modified multiferroic $BiFeO_3$ ceramics, J. Eur. Ceram. Soc. 30 (2010) 727–736.
[30] Q. Zhang, C.H. Kim, Y.H. Jang, H.J. Hwang, J.H. Cho, Oxygen concentration and its effect on the leakage current in $BiFeO_3$ thin films, Appl. Phys. Lett. 96 (2010) 012909–12911.
[31] C.-F. Chung, J.-P. Lin, J.-M. Wu, Influence of Mn and Nb dopants on electric properties of chemical-solution-deposited $BiFeO_3$ films, Appl. Phys. Lett. 88 (2006) 242909–242911.
[32] R.N.P. Choudhary, D.K. Pradhan, G.E. Bonilla, R.S. Katiyar, Effect of La-substitution on structural and dielectric properties of $Bi(Sc_{1/2}Fe_{1/2})O_3$ ceramics, J. Alloys Compd. 437 (2007) 220–224.
[33] X. Tang, H.L.-W. Chan, Effect of grain size on the electrical properties of $(Ba,Ca)(Zr,Ti)O_3$ relaxor ferroelectric ceramics, J. Appl. Phys. 97 (2005) 034109–34116.
[34] M. Idrees, M. Nadeem, M. Mehmood, M. Atif, K.H. Chae, M.M. Hassan, Impedance spectroscopic investigation of delocalization effects of disorder induced by Ni doping in $LaFeO_3$, J. Phys. D: Appl. Phys. 44 (2011) 105401–105412.